16th World Conference on Earthquake, 16WCEE 2017

Santiago Chile, January 9th to 13th 2017

Paper N° 1187

Registration Code: S-P1463347615

A GENERAL DESIGN METHOD FOR BUILDINGS WITH ENERGY DISSIPATION DEVICES

J.C. de la Llera[(1)], J. J. Besa[(2)]

[(1)] Professor, National Research Center for Integrated Natural Disaster Management CIGIDEN CONICYT/FONDAP/15110017 and Department of Structural and Geotechnical Engineering, Pontificia Universidad Católica de Chile, jcllera@ing.puc.cl
[(6)] M.Sc., Pontificia Universidad Católica de Chile, juanjosebesa@gmail.com

Abstract

A general design procedure for elastic buildings equipped with linear and non-linear energy dissipating devices is presented herein. The procedure begins with an estimation of the total amount of equivalent damping and stiffness required to achieve a predefined building performance. The method defines the modal significance of some key design performance indicators, and then focuses on the control of the modal properties by solving a singular two-parameter eigenvalue problem. Although simple, the definition of a new measure of modal significance in the classical and non-classical damping case, is also critical for faster convergence of the method. The incorporation of non-classical damping in the design algorithm appears to be critical, and expands its applicability significantly. The design output provides a target frequency shift and damping ratio for the complete structure, obtained from the so called iso-performance design curves (IPCs), which cover the whole design space spanned by these two design variables representing the supplemental stiffness and damping of the devices. Once the linear equivalent properties of the dampers are obtained, the equivalent stiffness and damping of the devices are transformed into parameters that characterize the inelastic force-deformation constitutive models of the physical dampers. The design procedure does not require any a-priori definition of a specific damper type. The design procedure was validated using 8 conventional buildings that were severely damaged during the February 27, 2010 Chile earthquake, and a rather complex free-plan building with two towers of a rhomboid-shape plan. Estimation errors between response reduction factors using linear versus inelastic modeling of the EDDs were usually less than 10% for the 9 buildings considered. The design procedure proposed is better described as a conceptual and practical framework for the design of buildings with passive EDDs. Its step-by-step nature can take advantage of future research in any of the current research topics described herein and could be easily adapted to new knowledge in the field.

Keywords: modal significance, energy dissipation devices, non-classical damping, iso-performance curves, optimal damping distribution.

1. Introduction

The successful performance of buildings equipped with seismic protection solutions during the recent cluster of large subduction earthquakes has generated increasing enthusiasm in using these techniques in the design of structures located in high seismicity environments. The response of thirteen seismically protected buildings during the Chile earthquake (Mw=8.8, 2010) [9], and many others during the Japan earthquake (Mw=9.0, 2011) [4][14] are just some examples of this successful behavior.

The literature in the topic of building design with EDDs is rather extensive [13][15] and deals with relevant aspects such as the optimal height-wise distribution location of EDDs [2][12] in single and multistory symmetric and asymmetric buildings; and the elastic and inelastic dynamic behavior of the building and their design considering different devices such as viscous, frictional, metallic, viscoelastic, and the more sophisticated semi-active dampers [e.g., 5].

This research proposes a general and robust procedure for the design of elastic buildings equipped with EDDs. Although elastic building behavior may seem initially as a limitation to the applicability of the procedure, three reasons justify this assumption. First, as it was observed during the Chile earthquake in 2010, the actual behavior of slender structures equipped with EDDs was predominantly linear-elastic. Second, being the linear case well understood, it is rather straightforward to extend this design procedure to account for the inelastic behavior of a building. And third, since this is a design procedure rather than an analysis procedure, the design generated can be validated in the end by any inelastic dynamic analysis of the structure including every possible nonlinearity. Consequently, this procedure should be understood as one possible algorithm to generate an optimal design.

This procedure formulates the design problem as one of reducing a key performance design index (KDPI) by analyzing and controlling the vibration "modes" of the structure. To achieve this, it is necessary to identify the relative contribution or significance that each generalized coordinate has on the response of the system. Any modal response is controlled through its modal dynamic parameters, its natural frequency and damping ratio. The target reduction for the modal response depends on the modal significance on the KDPI, which will be characterized by the *modal significance factor* (MSF) introduced later. Modal parameter changes will be measured by shifts in the natural frequency and supplemental damping ratio, characterized by the design pair (Ω^2, ξ_d), with Ω^2 and ξ_d as defined later. Modal parameter changes will be obtained from Iso-Performance Curves (IPCs), which represent the locus of all pairs (Ω^2, ξ_d) that produce the same response reduction of the KDPI. Regardless of the EDD finally used, linear equivalent properties are used in general to determine the shift in modal parameters.

Any KDPI may be represented by a response factor defined as the ratio $R_Z = Z_d/Z_0$, where Z_0 and Z_d are the peak responses of the bare and equipped structure with EDDs, respectively. A target value for this KDPI is defined in the design to quantify the effectiveness of the proposed solution. This target response reduction value is based largely on experience, but usually ranges between 20%-60% for practical building solutions. A convenient way to impose this design goal is through the use of the IPCs introduced later.

2. Formulation of the problem

The reduced order equations of motion of a linear-elastic structure can be stated as

$$\boldsymbol{M}_R\ddot{\boldsymbol{u}} + \boldsymbol{C}_R\dot{\boldsymbol{u}} + \boldsymbol{K}_R\boldsymbol{u} = \boldsymbol{\Psi}^T\boldsymbol{f}_g \tag{1}$$

where $\boldsymbol{u}$ is the vector of generalized coordinates; $\boldsymbol{\Psi}$ is a coordinate transformation matrix such that $\boldsymbol{x} = \boldsymbol{\Psi}\boldsymbol{u}$; and $\boldsymbol{M}_R = \boldsymbol{\Psi}^T\boldsymbol{M}\boldsymbol{\Psi}$, $\boldsymbol{C}_R = \boldsymbol{\Psi}^T\boldsymbol{C}\boldsymbol{\Psi}$, and $\boldsymbol{K}_R = \boldsymbol{\Psi}^T\boldsymbol{K}\boldsymbol{\Psi}$ are the mass, damping, and stiffness matrices in the new coordinate system, respectively; and $\boldsymbol{f}_g$ is a general input to the structure. The reduced order dynamic equations of the structure may be written in some cases, say the design of Tuned Mass Dampers (TMDs), as a combination of physical and generalized modal coordinates. In any case, the reduced order representation of the structure needs to be sufficiently accurate to capture a large percentage, say over 95%, of the target response. Thus, it is customary to select and adequate number of generalized coordinates by using the relative error of the response history of displacements and story-shears in the bare structure.

Key to the proposed design procedure is to control the modal (coordinate) responses of the structure. The target is to identify required variations in modal parameters that lead to a target KDPI. This problem is addressed in three steps: (i) identify the most relevant generalized coordinate in relation to the chosen KDPI; (ii) compute the response reduction of that coordinate; and (iii) compute the variations in the modal parameters that lead to the target reduction.

The steps of the algorithm to determine the reduction in response can be summarized as follows: (1) perform dynamic analysis of the reduced order model of the structure, ideally a response history analysis; (2) identify the peak response of the KDPI, say $Z(t^*)$, occurring at time t^*--for modal spectral analysis peak responses are used; (3) decompose this peak response at time t^* into modal contributions—in the case of classically damped systems this is straightforward, while in non-classically damped systems, uncoupling modes may be obtained as described elsewhere [6]; and (4) obtain for the *m-th* mode, the MSF χ_m by taking the ratio between the modal contribution and the peak response at t^*--i.e., given $Z(t^*)$ the peak response at time t^*, and $Z_m(t^*)$ the contribution of the *m-th* mode, χ_m is defined as:

$$\chi_m = \frac{Z_m(t^*)}{Z(t^*)} = \frac{Z_m(t^*)}{\sum_m Z_m(t^*)} \tag{2}$$

Please note that χ_m may have values with magnitude larger than 1, and that of all ratios, the most significant mode is defined as the one with the largest χ_m. The corresponding MSF will be denoted hereafter as χ_G.

In classically damped modal analysis, the modal decomposition of the response, $\boldsymbol{x} = \boldsymbol{\phi}\boldsymbol{q}$, where $\boldsymbol{\phi}$ and $\boldsymbol{q}$ are the natural modes and coordinates is straightforward and leads to the well- known set of *n* uncoupled equations of motion for mode $q_m(t)$, i.e.

$$\ddot{q}_m(t) + 2\xi_m\omega_m\dot{q}_m(t) + \omega_m^2 q_m(t) = \phi_m^T \boldsymbol{f}_g(t) \qquad m = 1, \dots, n \tag{3}$$

where ϕ_m is the *m-th* mode; and $x_m(t) = \phi_m\, q_m(t)$ is the *m-th* modal contribution to x. However, for non-classically damped structures, a more general approach is required [6], and the uncoupled equations of motion may be written as:

$$\ddot{q}_m(t) + 2\xi_m\omega_m\dot{q}_m(t) + \omega_m^2 q_m(t) = \boldsymbol{T}_{1m}^{\ T}\boldsymbol{f}_g(t) + \boldsymbol{T}_{2m}^{\ T}\dot{\boldsymbol{f}}_g(t) \qquad m = 1, \dots, n \tag{4}$$

where $\boldsymbol{f}_g$ and $\dot{\boldsymbol{f}}_g$ are the input and its time derivative, respectively. The modal parameters of the system result from solving the second order eigenvalue problem $(\boldsymbol{M}\lambda^2 + \boldsymbol{C}\lambda + \boldsymbol{K})\boldsymbol{\phi} = \boldsymbol{0}$, and as it is well known, the eigenvalues and eigenvectors appear in complex conjugate pairs. Although real modes may occur in an over-damped case, the procedure randomly pairs these real eigen-solutions and introduces them into the set of equations as conjugates pairs. Eigenvalues for this problem have the well-known structure of complex poles, i.e. $\lambda = -\xi\omega + j\omega\sqrt{1-\xi^2}$, with $(\lambda + \bar{\lambda}) = -2\xi\omega$, and $\lambda\bar{\lambda} = |\omega|^2$. Also, in Eq. (4), $\boldsymbol{T}_1 = [\boldsymbol{T}_{1m}]$ and $\boldsymbol{T}_2 = [\boldsymbol{T}_{2m}]$ are real matrices with its m-th columns $\boldsymbol{T}_{1m}$ and $\boldsymbol{T}_{2m}$. It can be shown that $\boldsymbol{T}_{1m} = (\boldsymbol{\phi}_m\bar{\lambda}_m - \bar{\boldsymbol{\phi}}_m\lambda_m)/(\bar{\lambda}_m - \lambda_m) = 2\mathrm{Re}\{\bar{\lambda}_m/(\bar{\lambda}_m - \lambda_m)\boldsymbol{\phi}_m\}$, and $\boldsymbol{T}_{2m} = (\bar{\boldsymbol{\phi}}_m - \boldsymbol{\phi}_m)/(\bar{\lambda}_m - \lambda_m) = 2\mathrm{Re}\{\boldsymbol{\phi}_m/(\lambda_m - \bar{\lambda}_m)\}$, while the m-th mode contribution to the response is given by $\boldsymbol{x}_m(t) = \boldsymbol{T}_{1m}q_m(t) + \boldsymbol{T}_{2m}\dot{q}_m(t) - \boldsymbol{T}_{2m}\boldsymbol{T}_{2m}^T\boldsymbol{f}_g(t)$. For example, if the KDPI is the maximum displacement of the building, i.e. $Z(t) = \max(\boldsymbol{x}(t))$), the MSF χ_m can be written for classically damped systems as:

$$\chi_m = \frac{Z_m(t^*)}{Z(t^*)} = \frac{\max(\boldsymbol{\phi}_m q_m(t^*))}{\max(\boldsymbol{\phi}\boldsymbol{q}(t^*))} \tag{5}$$

and for non-classically damped system as:

$$\chi_m = \frac{Z_m(t^*)}{Z(t^*)} = \frac{\max\left(\boldsymbol{T}_{1m} q_m(t^*) + \boldsymbol{T}_{2m}\dot{q}_m(t^*) - \boldsymbol{T}_{2m}\boldsymbol{T}_{2m}^T \boldsymbol{f}_g(t^*)\right)}{\max\left(\boldsymbol{T}_1 \boldsymbol{q}(t^*) + \boldsymbol{T}_2\dot{\boldsymbol{q}}(t^*) - \boldsymbol{T}_2\boldsymbol{T}_2^T \boldsymbol{f}_g(t^*)\right)} \tag{6}$$

If a reduction in dynamic order is used for design purposes, $\boldsymbol{x} = \boldsymbol{\Psi}\boldsymbol{u}$, as in Eq. (1), these MSF equations may be extended to include the coordinate transformation corresponding to the generalized modal matrix $\boldsymbol{\Psi}$, i.e.

$$\chi_m = \frac{\max(\boldsymbol{\Psi}\boldsymbol{\phi}_m q_m(t^*))}{\max(\boldsymbol{\Psi}\boldsymbol{\phi}\boldsymbol{q}(t^*))}, \text{ and } \chi_m = \frac{\max(\boldsymbol{\Psi}[\boldsymbol{T}_{1m} q_m(t^*) + \boldsymbol{T}_{2m}\dot{q}_m(t^*) - \boldsymbol{T}_{2m}\boldsymbol{T}_{2m}^T \boldsymbol{f}_g(t^*)])}{\max(\boldsymbol{\Psi}[\boldsymbol{T}_1 \boldsymbol{q}(t^*) + \boldsymbol{T}_2\dot{\boldsymbol{q}}(t^*) - \boldsymbol{T}_2\boldsymbol{T}_2^T \boldsymbol{f}_g(t^*)])} \tag{7}$$

for the classical (left) and non-classical (right) damped structure, respectively. Hence, the global modal significance ratio χ_G is defined as:

$$\chi_G = \max_m(\chi_m) \tag{8}$$

Most KDPIs, say story drifts or member forces, are obtained as linear combinations of several degrees of freedom (DOFs) of the structure, and the above equations need to be simply modified to introduce the corresponding output transformation matrices between the DOFs and the selected response.

Once the controlling mode has been selected (Eq. (8)), this mode controls the reduction of the KDPI until a second mode starts controlling, and the design procedure shifts to reduce incrementally the response of that second mode. Shown in Figure 1 is a schematic view of the algorithm, where χ_m is plotted against the response reduction R_Z for the first three controlling modes of a structure. Points A and B represent critical points where the controlling mode for the target response changes from the first to the second, and from the second to the third; the envelope corresponds to χ_G and is plotted in solid line. Because it is numerically costly in practice, and also unnecessary for design purposes, to determine the continuous variation of the response controlling mode as shown in Figure 1, the problem is numerically implemented by introducing reductions in one mode first, and if the intended reduction in response is not achieved, update the system matrices, recalculate all modes, and repeat the procedure with the new controlling mode until the target in response reduction is achieved.

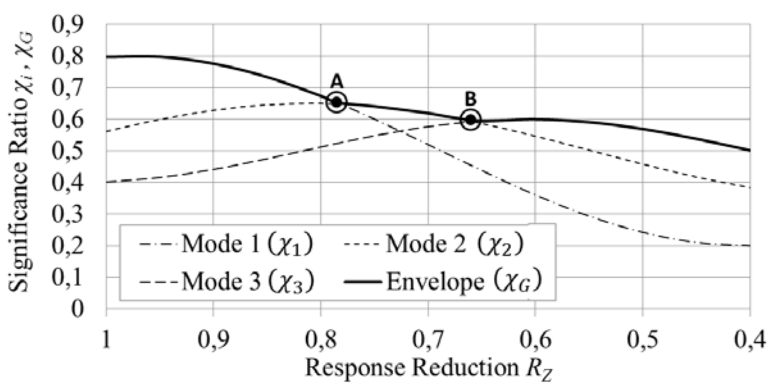

Fig. 1 – Variation of modal significance ratio (MSF) with global response reduction R_Z.

The reduction factor for the *m-th* controlling mode, R_m, needs to be defined by accounting for the effect of the other modes. Therefore, let $Z(t)$ be the response of interest, $Z_m(t)$ the contribution to $Z(t)$ of the *m-th* mode, and t^* the instant at peak value of the response. Then, $Z(t)$ is obtained as $Z(t^*) = \sum_m Z_m(t^*)$, and hence, the global reduction factor R_Z and the modal reduction factor R_m are related by $R_Z Z(t^*) = R_Z \sum_p Z_p(t^*) \approx R_m Z_m(t^*) + \left(\sum_p Z_p(t^*) - Z_m(t^*)\right)$, and solving for R_m

$$R_m \approx \frac{\sum_p Z_p(t^*)}{Z_m(t^*)}(R_Z - 1) + 1 = \frac{(R_Z - 1)}{\chi_G} + 1 \tag{9}$$

where $\chi_G = Z_m(t^*)/\sum_p Z_p(t^*)$. Please notice that Eq. (9) is an approximation since it assumes complete decoupling of the modes.

Theoretically, there are an infinite number of pairs of supplemental stiffness and damping that may lead to the same KDPI. The locus of these combinations is denoted herein as the IPC. When analyzing a single coordinate, supplemental stiffness and damping shift the modal frequency and damping ratio, and equal performance may be obtained by different pairs of these shifts denoted as (Ω^2, ξ_d). The IPCs enable us to define the total amount of supplemental stiffness and damping required to reduce the building response to a specific value. Using this total value, linear equivalent stiffness and damping parameters are obtained at each building story. The goal next is to guide the selection of the circular frequency shift and supplemental modal damping ratio required to achieve the desired modal response reduction R_m, i.e. the design pair (Ω^2, ξ_d) for the controlling mode, based on the dynamic properties of the bare structure.

Let us define the supplemental damping ratio $\xi_d = c_d/2m\omega_0$, where c_d is the modal linear equivalent viscous damping coefficient of the equipped structure; and $\Omega = \left((\omega_f/\omega_0)^2 - 1\right)^{1/2}$ the frequency shift, where ω_0 and ω_f are the circular natural frequencies of the bare and equipped structure (with EEDs), respectively. It is convenient to produce an appropriate parameterization of the problem by using modal analysis on the reduced order system with modal coordinate $\boldsymbol{q}$, such that $\boldsymbol{u} = \widetilde{\boldsymbol{\phi}}\boldsymbol{q}$, where $\widetilde{\boldsymbol{\phi}} = \left[\tilde{\phi}_m\right]$. External loads may be ground motions or a design spectrum. Derivations of the parametric representation are skipped and may be found elsewhere [1]. The resulting single coordinate equation of motion for the *m-th* controlling coordinate is:

$$\ddot{q}_m(t) + 2\xi_f\omega_f\dot{q}_m(t) + \omega_f^2 q_m(t) = \frac{\widetilde{\boldsymbol{\phi}}_m^T \boldsymbol{\Psi}^T \boldsymbol{f}_g(t)}{\widetilde{\boldsymbol{\phi}}_m^T \boldsymbol{M}_R \widetilde{\boldsymbol{\phi}}_m} \tag{10}$$

where $q_m(t)$ is the *m*-th generalized control coordinate of the system; and ξ_f and ω_f are the respective *m-th* coordinate damping ratio and natural frequency of the structure with EEDs. The natural frequencies and damping ratios of the equipped structure can be expressed in terms of the dynamic properties of the original bare structure parameters (ω_0, ξ_0) through the expressions:

$$\omega_f = \omega_0\sqrt{1+\Omega^2} \quad \text{and} \quad \xi_f = \frac{\xi_0 + \xi_d}{\sqrt{1+\Omega^2}} \tag{11}$$

It is apparent from Eq. (11) that the shape of the IPCs depends on the selected KDPI, the dynamic characteristics of the bare system (ω_0, ξ_0), and the input $\boldsymbol{f}_g(t)$. Shown as an example in Figure 2 are the displacement and acceleration IPCs corresponding to the NCh2745 design spectrum [10] for two different buildings with periods T_0=1s and T_0=3s, assuming an initial classical damping ratio for the bare structure ξ=0.05. Numerical labels on top of the IPC represent response reduction factors R_m, where 0.9 implies a 10% reduction, 0.6 implies a 40% reduction, and so forth. While IPCs differ for displacements and accelerations, especially for larger frequency shifts (Ω), in both cases 2(a) and 2(b), curves tend to be horizontal, which implies that introducing supplemental damping is more effective than reducing the response through stiffness. As Ω grows, stiffness is introduced into the system, and a larger damping ratio is needed to preserve the reduction in acceleration in the structure (Figures 2(a) and (b)).

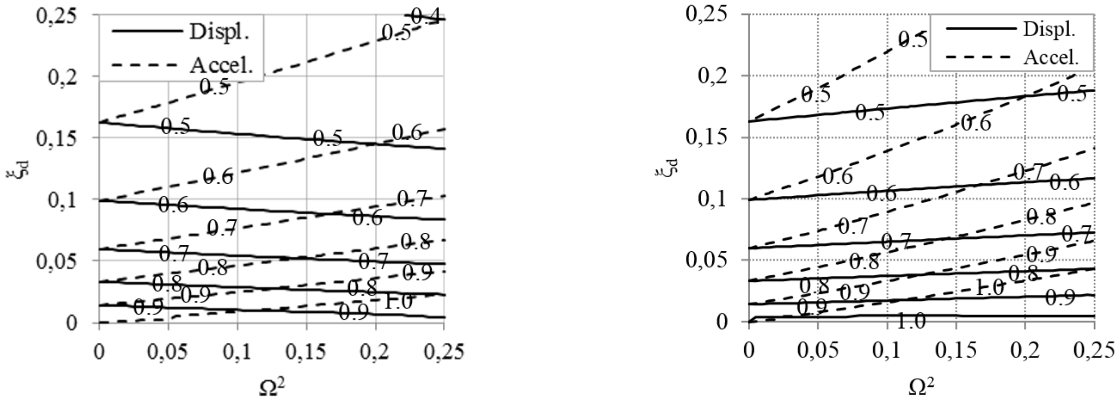

(a) T_0=1s (b) T_0=3s

Fig. 2 – IPCs for displacement and acceleration corresponding to the NCh2745 spectrum, soil type I (rock), and Seismic Zone 1

3. Heightwise distribution of EDDs

Numerous investigations have dealt with optimal damper distributions, and optimal criteria by selecting diverse objective functions [12]. Despite this effort, the question of which optimal criterion is better and why does not have a trivial and unique answer. Given a criterion, and optimal local solution is usually found. Moreover, the selection of an optimal damper distribution in a building is a three dimensional problem, and the optimal height-wise and plan-wise distributions are coupled. In the current procedure, the problem is split in two parts: (i) find an optimal height-wise distribution; and (ii) find a plan distribution that performs best for the already determined height-wise distribution. This is based on the fact that the 3D damper allocation problem may be dealt with by dynamically uncorrelating the lateral and torsional problem as explained elsewhere [2]. Furthermore, normalized stiffness and damping distributions $\boldsymbol{\alpha}$ and $\boldsymbol{\beta}$ are assumed proportional based on the case of metallic dampers. This assumption does not limit the generality of the design procedure and is used only for numerical convenience.

Although the design procedure may include any arbitrary height-wise distribution of supplemental dampers, the proposed strategy herein seeks a distribution of supplemental stiffness and damping that causes the highest perturbation of the dynamic properties of the controlled vibration mode given a fixed amount of total supplemental stiffness and damping. This problem is iterative in nature and requires and initial distribution to start with the iteration process. Theoretically, any initial distribution could be used, but due to numerical convergence it is advisable to choose it carefully.

The proposed initial distribution is obtained following the procedure described earlier, i.e. choosing the controlling mode based on the MSF χ_m. For each possible damper location l, compute the MSF χ_{l_d} corresponding to the d-th mode, and assume that the damper deformation is selected as the relevant response when χ_{l_d} is computed. Thus, the initial distribution vector proposed contains 0's in the damper locations not controlled by the mode controlling the KDPI, and 1's in those locations that are controlled by the mode. The final distribution vector is normalized to have unitary norm one. Consequently, as for χ_m in Eq. (8), χ_{l_d} can be written as:

$$\chi_{l_d} = \frac{\boldsymbol{L}_l\boldsymbol{\Psi}\left(\boldsymbol{\Phi}_d q_d(t_l^*)\right)}{\boldsymbol{L}_l\boldsymbol{\Psi}\left(\boldsymbol{\Phi}^T\boldsymbol{q}(t_l^*)\right)}, \text{ and } \quad \chi_{l_d} = \frac{\boldsymbol{L}_l\boldsymbol{\Psi}\left(\boldsymbol{T}_{1d} q_d(t_l^*)+\boldsymbol{T}_{2d}\dot{q}_d(t_l^*)-\boldsymbol{T}_{2d}\boldsymbol{T}_{2d}^T\boldsymbol{f}_g(t_l^*)\right)}{\boldsymbol{L}_l\boldsymbol{\Psi}\left(\boldsymbol{T}_1\boldsymbol{q}(t_l^*)+\boldsymbol{T}_2\dot{\boldsymbol{q}}(t_l^*)-\boldsymbol{T}_2\boldsymbol{T}_2^T\boldsymbol{f}_g(t_l^*)\right)} \tag{12}$$

for the cases of classical and non-classical damping, respectively; and $\boldsymbol{L}_l$ represents the row of the kinematic transformation matrix $\boldsymbol{L}$ corresponding to the location of the l-th damper. Thus, if the *m-th* mode is controlling the KDPI, then the *l-th* element of the initial guess distribution vector of EDDs, α_l (prior to normalization) is defined as:

$$\alpha_l = \begin{cases} 1, & if\ \chi_{l_m} = \max_d(\chi_{l_d}) \quad d = 1, \dots, n \\ 0, & otherwise \end{cases} \tag{13}$$

Once the initial distribution α_l has been defined by Eq. (13), the goal is to find the height-wise distribution of devices that requires the least value of total linear equivalent damping c_d. Linear equivalent properties, k_d and c_d are used for the dampers in order to define an initial design algorithm that is general to all devices [e.g., 11]. Furthermore, please assume without loss of generality that the *m-th* mode is the controlling mode, while ω_f and ξ_f are the target dynamic properties for that mode. However, the problem is cast somewhat in an inverse manner, given k_d and c_d as indicated elsewhere [1], find the height-wise distribution that leads to the largest modal damping ratio for the *m-th* mode.

For a certain distribution at the *k*-th iteration $\boldsymbol{\alpha}^{(k)}$, the overall supplemental linear equivalent parameters ${k_d}^{(k)}$ and ${c_d}^{(k)}$ are first determined from the solution of an eigenvalue problem as explained elsewhere [1,7,8]. A new distribution $\boldsymbol{\alpha}^{(k+1)}$ is obtained as the one that maximizes the modal damping ratio given ${k_d}^{(k)}$and ${c_d}^{(k)}$, i.e.,

$$\boldsymbol{\alpha}^{(k+1)} = \max_{\boldsymbol{\alpha}} \xi_m\left(\boldsymbol{\alpha}, c_d\left(\boldsymbol{\alpha}^{(k)}\right), k_d\left(\boldsymbol{\alpha}^{(k)}\right)\right), s.t. \quad \sum_l \alpha_l = 1, \quad 0 \le \alpha_l \le 1 \tag{14}$$

The procedure iterates until the variation in the height-wise damper distribution $\boldsymbol{\alpha}$, measured by the quadratic error, $e = \sqrt{\sum_{l=1}^{N}\left(\alpha_l^{(k+1)} - \alpha_l^{(k)}\right)^2 / N}$, becomes negligible. Hence, this Perturbation Based Optimal Distribution Algorithm (PBODA) is summarized as follows: (1) From Eq. (13), obtain an initial distribution of dampers $\boldsymbol{\alpha}^{(0)}$, select a desired tolerance, and set *k=0*; (2) determine ${k_d}^{(k)}$ and ${c_d}^{(k)}$ from the eigenvalue problem explained elsewhere using $\boldsymbol{\alpha}^{(k)}$; (3) compute from Eq. (14) an updated distribution $\boldsymbol{\alpha}^{(k+1)}$; and (4) if the tolerance is not reached, set *k*=*k*+1 and iterate to Step 1; otherwise, set $\boldsymbol{\alpha} = \boldsymbol{\alpha}^{(k)}$ and exit. Numerical aspects of the solution of the above algorithm can be found elsewhere [1].

4. Validation of the design algorithm

A summary of the results of applying the proposed design procedure to 8 shear wall buildings that underwent structural damage during the February 27, 2010 Chile Earthquake is presented in this section [16][17]. Herein, X- and Y-directions refer to the principal building axes. Please note that each buildings PP-7 and RT-8 are composed by two different blocks, separated by a construction joint, so tables differentiate these blocks by indices “a” and “b”. Shown in Table 7 is a summary of the total equivalent supplemental damping and stiffness required for each of the buildings in order to achieve the nominal target response reduction $R_Z=0.6$.

Because the structural configurations of these buildings are quite simple, the complete design procedure ended after one or two iterations (last column, Table 2), and in most cases the damper capacity was rather concentrated in few stories. Indeed, several of these distributions locate dampers in a single story, such as the case for the X-direction distributions of AA-1, AH-2, CM-3, TL-4, PP-7a, and TO-9. This result is in complete agreement with the modal distribution theorem presented elsewhere [1]. Please notice that the damper capacity values presented in this table are relatively small when compared with damping values required in larger structures with lateral stiffnesses much larger.

Table 1 – Comparison of the responses and reduction factors between linear equivalent analysis and results obtained using the nonlinear force-deformation and force-velocity constitutive relationships—numbers in parenthesis represents de ratio between nonlinear and linear cases (target $R_Z \le 0.6$)

Direction	Linear Equivalent			TADAS		Non-linear viscous	
	$Z_0\ (cm)$	$Z_F\ (cm)$	R_Z	$Z_F\ (cm)$	R_Z	$Z_F\ (cm)$	R_Z

X	52.467	30.91	0.589	25.99 (84.0%)	0.495	30.31 (98.1%)	0.578
Y	49.063	28.12	0.573	32.31 (114.9%)	0.659	27.45 (97.6%)	0.559

Table 2 – Summary of the total linear equivalent supplemental damping and stiffness required to achieve a response reduction factor $R_Z \leq 0.6$

Building	**Period T (s)**	**Equivalent Damping c_d (ton s/cm)**			**Equivalent stiffness k_d (ton/ cm)**			**Design Iterations X ; Y**
		X	**Y**	R_Z	**X**	**Y**	R_Z	
AA-1	0.71	4.06	3.67	0.59	18.61	21.91	0.60	1 ; 1
AH-2	0.70	6.31	10.39	0.59	43.18	125.88	0.42	1 ; 2
CM-3	0.80	6.99	3.01	0.62	44.25	22.48	0.58	1 ; 1
TL-4	0.77	2.95	1.43	0.58	15.06	7.94	0.58	1 ; 1
PR-6	0.50	1.73	2.03	0.56	11.20	21.22	0.56	1 ; 1
PP-7a, RT-8a	0.36	3.85	1.49	0.59	40.38	22.17	0.59	1 ; 1
PP-7b, RT-8b	0.34	2.98	1.52	0.54	55.42	16.93	0.58	1 ; 1
TO-9	0.93	1.70	6.50	0.58	8.04	39.40	0.55	1 ; 1

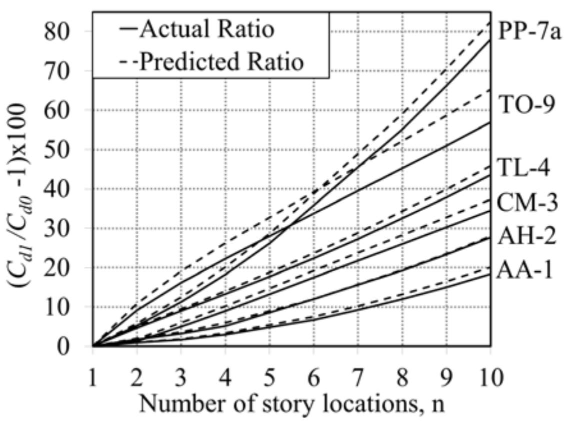

(a) Linear Distribution

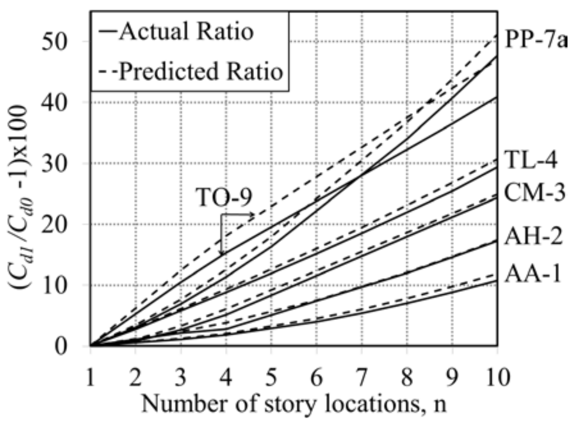

(b) Quadratic Distribution

Fig. 3 – Required increase in total linear equivalent damping using "*n*"-number of additional dampers locations, and considering two types of distribution

To evaluate the impact of the height-wise distributing of EDDs, the damper capacity and stiffness required was spread in several stories. As stated earlier, stories were organized in descending order of deformation demand on the EDDs, and a linear and quadratic height-wise damper distributions were tested. This is to understand the loss in efficiency of damper distributions in case we want to avoid excessive concentration of damper capacity in few stories. Ratios of the required increase in linear equivalent damping to achieve the same response reduction factor R_Z are shown in Figure 3, and compared with the expected values derived theoretically. It is apparent that there is always a loss in efficiency as we distribute damper capacity in more stories. Consequently, the solutions presented in Table 2 are locally optimal. The quadratic distribution of damper capacity shows an inefficiency smaller than the linear case, which is obvious since more damping is placed where the highest EDD drift location occurs. As it was said earlier, in most practical cases localizing damping is impractical since it implies large forces, and hence, eventual problem with the joints and connections. As shown in this Figure, the accuracy of the analytical prediction is acceptable and conservative for the whole range of stories considered in the distribution of damping.

Table 3 – Summary of the maximum response reduction R_Z for the eight buildings using three ground acceleration records (Chile, 1985) (Target $R_Z \leq 0.6$).

Building	Response Reduction, R_Z X-, Y-Direction		
	San Felipe	Melipilla	Llolleo
AA-1	0.59, 0.60	0.65, 0.72	0.59, 0.65
AH-2	0.59, 0.42	0.65, 0.43	0.64, 0.44
CM-3	0.62, 0.58	0.59, 0.75	0.62, 0.64
TL-4	0.58, 0.58	0.63, 0.81	0.60, 0.71
PR-6	0.56, 0.58	0.53, 0.61	0.55, 0.65
PP-7a, RT-8a	0.59, 0.59	0.59, 0.66	0.58, 0.61
PP-7b, RT-8b	0.54, 0.58	0.55, 0.60	0.53, 0.61
TO-9	0.58, 0.55	0.83, 0.60	0.70, 0.59

Table 4 – Y-Direction inelastic response history analysis of the buildings subject to the San Felipe record (Chile, 1985).

Building	Y-Direction				
	$Z_0\,(cm)$	TADAS		Viscous	
		$Z_F\,(cm)$	R_Z	$Z_F\,(cm)$	R_Z
AA-1	22.52	11.49	0.61	13.46	0.60
AH-2	17.31	10.36	0.60	8.35	0.48
CM-3	24.12	8.99	0.59	14.99	0.62
TL-4	25.14	11.47	0.58	15.86	0.63
PR-6	7.18	8.82	0.60	4.63	0.64
PP-7a, RT-8a	6.57	1.83	0.66	4.33	0.66
PP-7b, RT-8b	9.51	2.11	0.66	6.05	0.64
TO-9	18.20	25.17	0.61	10.97	0.60

Although the design of the 8 buildings was performed using an spectrum compatible ground motion from the seed record of San Felipe (Chile, 1985), a time history analysis was also performed using the same design for two other design spectrum compatible records based on the seed records of Melipilla and Llolleo (Chile, 1985). Shown in Table 3 is a summary of these results, and though the design based on the San Felipe record leads to quite reasonable results, a better solution is obtained when the average of the design for several ground motions is used to extrapolate among cases. If the lateral displacements of a building are coupled in both lateral directions such as in AH-2, the required supplemental stiffness and damping design in one direction leads to a larger response reduction as a result of the effect of the equivalent stiffness and supplemental damping defined in the orthogonal direction.

Finally, shown in Table 4 is a comparison of the results of non-linear response history analyses for the 8 buildings equipped with either TADAS or non-linear viscous dampers with velocity coefficient α=0.8. It is apparent that the procedure works very well, though some of the nonlinear results show reduction factors slightly above the target value $R_Z = 0.6$. They could be improved easily by a small modification of the design, but the results prove again that for design purposes the linear equivalent method proposed herein works well when compared against the building response with inelastic dampers.

5. Conclusions

A general design framework for elastic structures with inelastic supplemental damping is proposed herein. The procedure seeks modal control by first obtaining the total amount of equivalent damping and stiffness to achieve a specific building performance. Then, it sweeps the whole design space spanned by two design variables representing a shift in natural frequency and damping ratio (IPCs). For the sake of validation, the study considers 8 shear wall buildings damaged during the 2010 Chile earthquake. It was observed that in all cases, the procedure led in one or two iterations to an optimal design ($R_Z \leq 0{,}6$) of the EDDs. The incorporation of non-classical damping in the design algorithm becomes critical and expands its applicability significantly. Although very simple, the definition of a new measure of modal participation, the *Modal Significance Factor (MSF)*, in the classical and non-classical damping case is also critical for faster convergence of the method.

It is also concluded that though linear equivalent methods are controversial in their usefulness to predict inelastic responses, they are still very useful as a design tool. The main advantage is that they provide a completely general framework for the design of EDDs. No a-priori definition of a specific damper type is required, and estimation errors between response reduction factors using linear versus inelastic models for the EDDs are usually less than 10% in the buildings considered.

Optimal designs tend to concentrate damping in a few stories, and in several cases in a single story. This is in perfect agreement with theory, but inconvenient from a practical standpoint. In practice, this optimal solution can be perturbed slightly to better distribute damping and stiffness in several stories according to a rule that ranks stories in descending order of deformation demand for the EDDs.

The design procedure proposed is better described as a conceptual and practical framework for the design of buildings with passive EDDs. Its step-by-step nature can take advantage of future research in any of the pending topics presented herein and could be easily adapted to new knowledge in the field.

Acknowledgements

This research has been funded by Grants CONICYT/ Fondecyt/1141187, CONICYT/ FONDAP/15110017 (National Research Center for the Integrated Management of Natural Disasters, CIGIDEN), and CONICYT/ Doctorado Nacional/2013. The authors are very grateful for this support and that of the many collaborators that preceded this manuscript, especially Ricardo Uliarte and Ian Watt.

References

1. Besa, J.J. (2012). Master of Science Thesis, Effective Design Procedure of Buildings with Energy Dissipation Devices. Pontificia Universidad Católica de Chile.
2. De la Llera, J. C., Chopra, A. K., & Vial, I. J. (2005, July). Torsional balance of plan-asymmetric structures with frictional dampers: analytical results. *Earthquake Engineering and Structural Dynamics, 34*(9), 1089-1108.
3. De la Llera, J. C., Esguerra, C., & Almazán, J. L. (2003). Earthquake behavior of structures with copper energy dissipators. *Earthquake Engineering & Structural Dynamics, 33*(3), 329-358.
4. Li Meng, Q. (2011). Bridges Damage during East-Japan Earthquake on 11th March 2011. *Applied Mechanics and Materials, Advances in Civil Engineering*(90-93), 1649-1658.
5. Lin, W.-H., & Chopra, A. K. (2002). Earthquake response of elastic SDF systems with non-linear fluid viscous dampers. *Earthquake Engineering and Structural Dynamics, 31*(9), 1623-1642.
6. Ma, F., Morzfeld, M., & Imam, A. (19 de July de 2010). The decoupling of damped linear system in free or forced vibration. *Journal of Sound and Vibration, 329*(15), 3182-3202.

7. Muhic, A., & Plestenjak, B. (2009). On the Singular Two-Parameter Eigenvalue Problem. *Electronic Journal of Linear Algebra*, *18*, 420-437.
8. Muhic, A., & Plestenjak, B. (2010). On the Quadratic Two-Parameter Eigenvalue Problem and its Linearization. *Linear Algebra and its Applications, 432*, 2259-2542.
9. Naeim, F., Lew, M., Carpenter, L. D., Youssef, N. F., Rojas, F., Saragoni, G. R., & Schachter Adaros, M. (2011). Performance of tall buildings in Santiago, Chile during the 27 February 2010 offshore Maule, Chile earthquake. *The Structural Design of Tall and Special Buildings, 20*(1), 1-16.
10. NCh 2745. (2003). *Análisis y Diseño de Edificios con Aislación Sísmica.* Santiago, Chile: Instituto Nacional de Normalización.
11. Park, J.-H., Min, K.-W., Chung, L., Lee, S.-K., Kim, H.-S., & Moon, B.-W. (2007). Equivalent linearization of a friction damper-brace system based on the probability distribution of the extremal displacement. *Engineering Structures*, *29*(6), 1226-1237.
12. Singh, M. P., & Moreschi, L. M. (2002). Optimal placement of dampers for passive response control. *Earthquake Engineering & Structural Dynamics*, *31*(4), 955-976.
13. Soong, T. T., & Spencer, B. F. (2002). Supplemental energy dissipation: state-of-the-art and state-of-the-practice. *Engineering Structures, 24*(3), 243-259.
14. Takewaki, I., Murakami, S., Fujita, K., Yoshitomi, S., & Tsuji, M. (2011). The 2011 off the Pacific coast of Tohoku earthquake and response of high-rise buildings under long-period ground motions. *Soil Dynamics and Earthquake Engineering, 31*(11), 1511-1528.
15. Watt, I. (2006). *Performance Based Design with Energy Dissipation Devices for Passive Control of Nominally Symmetric Structures.* Santiago: School of Engineering, Pontificia Universidad Católica de Chile.
16. Westenenk, B., De la Llera, J. C., Besa, J. J., Jünemann, R., Moehle, J. P., Lüders, C., . . . Hwang, S. J. (2012). Response of Reinforced Concrete Buildings in Concepción during the Maule Earthquake. *Earthquake Spectra. Accepted for publication*.
17. Westenenk, B., De la Llera, J. C., Jünemann, R., Hube, M., Besa, J. J., Lüders, C., . . . Jordán, R. (2012). Analysis and Interpretation of the Seismic Response of RC Buildings in Concepción during the February 27 2010 Chile Earthquake. *Bulletin of Earthquake Engineering. Submitted 2012.*